Sector and Site Switch-Off Regular Patterns for Energy Saving in Cellular Networks

Tamer Beitelmal, *Student Member, IEEE,* Sebastian S. Szyszkowicz, *Member, IEEE,* David González G., *Member, IEEE,* and Halim Yanikomeroglu, *Senior Member, IEEE*

***Abstract*—Strategically switching off cells in off-peak times is an important way to reduce the energy consumption in cellular networks. Choosing which cells to switch off when is a research topic known as cell switch-off (CSO). Whereas *online* CSO approaches, based on immediate user demands and channels states, are problematic to implement and difficult to model, *offline* CSO approaches are more realistic and tractable for saving energy. Furthermore, it is known that regular cell layouts generally provides the best coverage and spectral efficiency, which leads to a significant preference by the research community for regular static (offline) CSO. In this context, sector-based CSO offers additional opportunities for energy saving that has not been well explored.**

In this paper, we consider several typical regular CSO patterns over a regularly laid-out cellular network with three-sector antennas, and we combine these patterns with sector-level switch-off to create even more regular patterns (42 in total). We compare these patterns in terms of their energy consumption and average number of users supported. We show that the average number of users can be captured by one parameter. Moreover, we find that the distribution of the number of users is close to Gaussian, with a tractable variance. Our results demonstrate that several patterns that switch on only one out of three sectors (the same sector in each cell) are particularly beneficial and less complex; such CSO patterns have not been studied before.

***Index Terms*—Green Communications, LTE, Cell Switch-Off (CSO), Offline CSO, Regular Static CSO, CSO Patterns, Sectorized CSO Patterns.**

I. Introduction

Fifth generation (5G) wireless networks are expected to support up to 1,000-fold gains in capacity. Several sophisticated techniques are to be employed to achieve this ambitious target. A key enabler is network densification by installing more small cells, which can be seen as bringing the network closer to the user equipment (UE) to improve its received power [1]. On top of network densification, aggressive frequency reuse is applied to efficiently utilize the scarce spectrum.

T. Beitelmal, S. S. Szyszkowicz and H. Yanikomeroglu are with the Department of Systems and Computer Engineering, Carleton University, Ottawa, Ontario, Canada. (e-mail: {tamer, sz, halim}@sce.carleton.ca).

D. González G. is with the Department Communications and Networking, Aalto University, Finland. (e-mail: david.gonzalez.g@ieee.org).

Although it promises to achieve higher rates, installing more cells means more energy consumption. This is because base stations (BSs) consume 50-80% of the total energy in a cellular network [2], [3]. This amount is not proportional to the load level at a cell, i.e., a non-loaded cell will consume approximately the same energy as a fully-loaded one [4], [5]. This increase in energy consumption conflicts with the energy efficiency targets of 5G networks.

An effective approach to meet these targets is to entirely switch off some cells in periods of low traffic and distribute their UEs to neighbouring cells . This approach, known as cell switch-off (CSO), aims at reducing energy consumption without sacrificing the quality of service (QoS) or the coverage area. Although relatively new, several CSO approaches have been proposed to tackle CSO issues from different angles (see survey papers [6], [7] for details).

One important issue in CSO is interference modeling, which is challenging because it is hard to know the set of active cells a priori. Typically, UEs are connected to the best sector in terms of downlink signal-to-interference-plus-noise ratio (SINR). However, when switching off a cell, its UEs need to be reassigned to another, perhaps less advantageous, cell. Without a proper interference characterization, these UEs might encounter a large amount of interference, because the set of active cells that contribute to the interference is only known at the final stage; and hence, resulting performances are not accurate. Indeed, some approaches assume zero interference, i.e., there is a perfect inter-cell interference coordination (ICIC) [4], [8]. This assumption is too optimistic and produces unachievable upper bound on the number of switched-off cells. Other approaches assume full interference, i.e., all cells are active all the time [9]. This assumption yields a poor lower bound on the number of switched-off cells.

One accurate way to model interference, thus alleviating the aforementioned problem, is by predetermining the set of active cells, i.e., the cells that actually generate the interference in the system. This is sometimes referred to as offline or static CSO [6], [7]. It is possible to predetermine several sets of active cells for different traffic densities and then select an appropriate set to accommodate the specific traffic distribution.

Regular static CSO (CSO patterns) is a special case of static CSO, where active BSs are predetermined such that their locations form a cellular layout that is as regular as possible [7]. It was shown that, for the same number of BSs, the best SINR distribution can be achieved

when the BSs are located in a regular grid [10]. Since, CSO patterns were introduced in literature to make the interference tractable and to avoid coverage holes at the same time. The possibility of successfully adopting regular CSO patterns is investigated in this paper; our results confirm positively this hypothesis as it will be shown later on.

Regular CSO patterns are based on a logical AND combination of site-level and sector-level patterns. We compare the performance of these patterns using only one parameter, abstracting from bandwidth and required rate. We provide an illustrative example to compare different patterns in terms of number of UEs supported, downlink SINR distribution, and power consumption. In most cases, patterns where one third of the sectors are active (each time with the same orientation) can support the most UEs per sector, due to a favourable interference scenario. Beside the items described above, this paper's major contributions are:

- Investigating regular CSO patterns with sector switching off, the first paper to do so.
- Providing a systematic way to predict the average number of users that each pattern can support using only one metric, the equivalent spectral efficiency (ESE).
- Finding that the distribution of the number of UEs supported closely follows a Gaussian distribution, whose variance can be estimated.

This paper is organized as follows: Section II classifies the different CSO approaches. Section III provides the mathematical methodology and introduces different CSO patterns and studies their power consumption. Section IV describes the simulation setup, while Section V provides a comparative case study, showing the number of users supported. Section VI concludes the paper.

II. CSO Classifications

There are two main CSO categories: online and offline. In CSO literature, BSs are usually distributed on a regular grid, often triangular, sometimes square. Switching off individual sectors is highlighted in the last subsection.

A. Online CSO

In this case, an algorithm is executed in real time to determine the set of cells to be switched off. This requires global knowledge about the channel state information between each UEs and all cells, as well as the load level of all cells in the network. It is difficult for this vast amount of information to be exchanged by the network in a timely manner [6]. The computational time might also be prohibitive for large networks. As mentioned earlier, another challenge in online CSO is interference modeling, due to the unpredictable set of active cells.

Online CSO is also known as dynamic CSO [7]. Online CSO is further classified as fast reaction or slow reaction.

1) Fast Reaction Online CSO: These algorithms are able to adapt quickly to changes in the current traffic and attempt to provide optimal energy saving [11]. This category allows for a fast change in the network configuration (a few seconds at most).

2) Slow Reaction Online CSO: In this case, the change in network configuration requires a relatively longer time and only allows for long term changes (tens of seconds to minutes). These algorithms operate based on the average traffic measures or available traffic statistics, usually relying on certain traffic pattern recognition capabilities.

Another important obstacle towards the practical implementation of online CSO is the time required for the on/off switching and for completing the UEs handover procedure [12].

B. Offline CSO

In this case, different sets of active cells are predetermined offline, and the operator determines the appropriate set to accommodate the current traffic density [13]. Only information related to the predetermined set of active cells is needed. Offline CSO is usually applicable for longer times (hours) and often based on historical load distribution.

Offline CSO is also known as static CSO [7]. Offline CSO is further classified as static or regular static.

1) Static CSO: It is different from online CSO because the network configuration will remain static for the specific period of time. Therefore, the interference can be modeled appropriately (in statistical terms) by including only the predetermined set of active cells [5].

Static CSO can be seen as a cell planning problem, but with a constrained set of BS locations. While in cell planning, the cell location is based on a wider set of possible locations, here the locations are restricted to actual sites of BSs, from which a subset is chosen to be active.

2) Regular CSO: This is a special case of static CSO, also known as CSO patterns. Besides being predetermined offline, the set of active cells is selected so that they are located within a periodic pattern [7]. Regular CSO patterns resemble the intuitive frequency reuse patterns [14]. In this paper, we propose regular CSO patterns as a mean to leverage the advantages of a regular topology (good SINR and coverage) [10].

By applying regular CSO, the choice of active cells minimizes the coverage holes. This aspect is usually overlooked in the literature [15]. Also, it is more energy-efficient for UEs when there is always a nearby cell [16]. Regular CSO patterns can reduce the interference among cells due to the careful selection of BS locations to be as far from each others as possible. The patterns are conceptually simple and easy to describe in a systematic way.

CSO Patterns is already under consideration by several research groups. Table I summarizes the existing work on regular CSO patterns. The effect of different CSO patterns on the outage probability is investigated in [13], [14], while

Table I
Regular CSO Patterns in Literature.

Ref.	Network	CSO Pattern Layout	
		Hexagonal	Square
[13]	CDMA	$\frac{1}{4}$	—
[14]	Generic	$\frac{2}{3}$, $\frac{2}{4}$, $\frac{3}{7}$	—
[17]	UMTS	—	$\frac{1}{2}$ $\frac{1}{2}$, $\frac{2}{3}$, $\frac{1}{4}$, $\frac{1}{9}$
[20]	OFDMA-based	$\frac{1}{4}$, $\frac{1}{7}$	$\frac{1}{4}$, $\frac{1}{9}$
[18]	UMTS	$\frac{1}{3}$, $\frac{1}{4}$ ($\frac{1}{7}$, $\frac{1}{9}$)	—
[21]	UMTS	$\frac{1}{4}$, $\frac{1}{7}$ $\frac{1}{9}$	$\frac{1}{2}$, $\frac{2}{3}$, $\frac{1}{9}$, $\frac{1}{5}$
[19]	LTE Macro	$\frac{1}{3}$, $\frac{2}{3}$, $\frac{1}{4}$, $\frac{2}{4}$, $\frac{3}{4}$	—
[22]	Release 10	$\frac{1}{4}$, $\frac{2}{4}$, $\frac{3}{4}$	—

Table II
List of Symbols

W	total system bandwidth.
N	number of UEs that can be served per active sector.
γ_i	SINR between UE i and its serving sector.
η_i	spectral efficiency of UE i, $= \log_2(1+\gamma_i)$ (bps/Hz).
R_i	rate required by UE i.
b_i	bandwidth required by UE i, $= R_i/\eta_i$ (Hz).
η_{eq}	equivalent spectral efficiency (ESE), $= 1/\mathbb{E}\{1/\eta\}$ (bps/Hz/Sector).
$\mathsf{P}_{\mathrm{X}}(n/m, k/3)$	CSO pattern where n out of m BSs are active, k out of 3 sectors are active, and X is to distinguish between different rotations.
ρ	proportion of active sectors in the network, $= \lvert\mathsf{P}(n/m, k/3)\rvert = \frac{nk}{3m} \in [0,1]$.
P_{site}	is the power consumed at a site.
P_S	the power consumed per each sector.
P_C	the common power consumed at a site.
α	$= P_S/P_C$.
δ	ratio of ESEs of two patterns.
P_o	probability of signal outage, when $\gamma_i < -7$ dB.
$\mathbb{C}\mathrm{oV}\{X\}$	coefficient of variation of a random variable X $= \sqrt{\mathbb{V}\mathrm{AR}\{X\}}/\mathbb{E}\{X\}$.

the effect on the blocking probability is studied in [17], [18]. Authors in [19] introduce a set of CSO patterns and propose a scheduler to jointly ensure full coverage for both downlink and uplink.

C. Hybrid CSO

For best system performance, it might be necessary to have a hybrid CSO approaches, where an online CSO algorithm is executed on top of the offline one. Hybrid approaches have a set of static cells to provide coverage and collect network information; those cells are never switched off. The remaining cells participate in an online CSO algorithm to accommodate the variability in UEs demand [13].

D. Switching Off Sectors

Most of the research in online CSO is executed in a sector-based manner, i.e., each sector can be turned off individually [5], [9]. To the best of our knowledge, this is not the case for regular CSO patterns, where only the entire BS is turned off; i.e., individual sector switch off is not considered in literature.

In the rest of this paper, we show that regular CSO patterns with individual sector switch-off can be efficient in several interesting cases. Each BS site has three 120°-sectors. The azimuth orientation of the sectors is the same for all sites.

III. Methodology

In this section we introduce the mathematical methodology and notation we follow to compare different CSO patterns. The symbols used are provided in Table III.

A. Performance Metrics

In this subsection, we study the distribution of the number of UEs served by an active sector and derive expressions for the average number of UEs $\mathbb{E}\{N\}$ and the variance.

In order to find the number of UEs N that can be served by an active sector, we formulate the problem using renewal theory [23, Chapter 7]. We assume that the UEs are admitted to the network on a first-come first-served basis regardless of their bandwidth demand:

$$b_i = \frac{R_i}{\eta_i}, \tag{1}$$

which depends on the UE's downlink rate requirement R_i, and its downlink spectral efficiency η_i. UEs are admitted one-by-one, their bandwidth requriment are added up until the next UE exceeds the downlink bandwidth W. Thus we have:

$$\begin{aligned} &\sum_{i=1}^{N} b_i \leq W, \text{ and} \\ &\sum_{i=1}^{N+1} b_i > W. \end{aligned} \tag{2}$$

Since $\{b_1, b_2, ..., b_N, b_{N+1}\}$ is a sequence of positive independent and identically distributed random variables, the renewal process $N(w)$ can be defines as:

$$N(w) = \max\left\{N \in \mathbb{N} : \sum_{i}^{N} b_i \leq w\right\}. \tag{3}$$

If we take W as the stopping time of this renewal process, we find that $N(W) = N$ is the number of UEs that will be admitted by one active sector.

1) Equivalent Spectral Efficiency: From the Central Limit Theorem for renewal processes: for large W, $N(W)$ is approximately normally distributed with approximate mean $W/\mathbb{E}\{b\}$, where

$$\mathbb{E}\{b\} = \mathbb{E}\left\{\frac{R}{\eta}\right\} = \mathbb{E}\{R\}\mathbb{E}\left\{\frac{1}{\eta}\right\}, \tag{4}$$

since R_i and η_i are independent random variables. Then

$$\mathbb{E}\{N\} \cong \frac{W}{\mathbb{E}\{R\}}\eta_{eq}\,, \tag{5}$$

where η_{eq} is the ESE, and is calculated as:

$$\eta_{eq} = \frac{1}{\mathbb{E}\{1/\eta\}} \text{ (bps/Hz/Sector)}. \tag{6}$$

The average number of UEs $\mathbb{E}\{N\}$ is also close to the median (50%) value, because of the symmetry of the Gaussian distribution.

η_{eq} is an interesting metric as it predicts the pattern performance abstracting from the bandwidth and the rate. It is obtained from simulation by simulating many UEs in the network and considering the spectral efficiency of the ones which select sector 1 as their best serving sector based on downlink SINR.

2) SINR Range: Among the UEs that select to be connected to sector 1, some of them might have a very weak SINR ($< \gamma_{min}$); at this value, the UE cannot receive any useful communication. Therefore, these UEs are removed and considered when estimating the outage probability P_o. Other UEs will have very high SINR ($> \gamma_{max}$), which are higher than what the current constellations can utilize; therefore, these SINRs are truncated. For LTE networks, typical values for γ_{min} and γ_{max} are -7 dB and 18 dB respectively [24], [25].

3) Variance and Distribution of Number of Users: Similarly, from the same Central Limit Theorem, the variance of $N(W)$ is approximated by $W\,\mathbb{VAR}\{b\}/\mathbb{E}^3\{b\}$.

$$\mathbb{VAR}\{N\} \cong \frac{W\,\mathbb{VAR}\{b\}}{\mathbb{E}^3\{R\}\mathbb{E}^3\{1/\eta\}}\,, \tag{7}$$

where

$$\begin{aligned}\mathbb{VAR}\{b\} &= \mathbb{VAR}\left\{\frac{R}{\eta}\right\}\\ &= \mathbb{VAR}\{R\}\mathbb{VAR}\left\{\frac{1}{\eta}\right\}\\ &+ \mathbb{VAR}\{R\}\mathbb{E}^2\left\{\frac{1}{\eta}\right\}\\ &+ \mathbb{E}^2\{R\}\mathbb{VAR}\left\{\frac{1}{\eta}\right\}.\end{aligned} \tag{8}$$

After some simplifications we obtain

$$\begin{aligned}\mathbb{VAR}\{N\} \cong\, &\mathbb{E}\{N\}\mathbb{CoV}^2\left\{\frac{1}{\eta}\right\}\\ &\times\left(\mathbb{CoV}^2\{R\} + \frac{\mathbb{CoV}^2\{R\}}{\mathbb{CoV}^2\{1/\eta\}} + 1\right),\end{aligned} \tag{9}$$

where the coefficient of variation of a random variable X is defined as $\mathbb{CoV}\{X\}$
$= \sqrt{\mathbb{VAR}\{X\}}/\mathbb{E}\{X\}$.

For fixed UE rate requirement R, the variance simplifies to

$$\mathbb{VAR}\{N\} \cong \mathbb{E}\{N\}\mathbb{CoV}^2\left\{\frac{1}{\eta}\right\}. \tag{10}$$

Since the distribution of $N(W)$ is approximately Gaussian, we now know the approximate distribution of N. Thus, for example, the number of UEs we can support 97.5% of the time is approximately

$$\begin{aligned}&\mathbb{E}\{N\} - 1.96\sqrt{\mathbb{VAR}\{N\}}\\ =&\mathbb{E}\{N\} - 1.96\sqrt{\mathbb{E}\{N\}}\mathbb{CoV}\left\{\frac{1}{\eta}\right\},\end{aligned} \tag{11}$$

where 1.96 comes from the Gaussian table for the 97.5% area of the normal distribution.

B. Site-Level CSO Patterns

We define 14 different site-level regular CSO patterns, where only entire BSs are switched off (i.e., there is no individual sector switch-off). Most of these patterns appear in regular CSO literature (see Table I).

The pattern for which all BSs are active (without CSO) is called $\mathsf{P}(1)$. Then $\mathsf{P}(n/m)$ is the pattern where n out of every m BSs are active; the proportion of active cells in these patterns is $\rho = \frac{n}{m}$. Some patterns have special rotation cases, where for the same $\frac{n}{m}$, there are different possible rotations. To differentiate between those rotations, patterns are referred to as $\mathsf{P}_\mathrm{X}(n/m)$, where the subscript X denotes a particular rotation.

Fig. 1 shows the different possible patterns we investigate at this level. Those patterns are based on the well-known frequency reuse patterns, where m is the number of BSs in the reuse cluster. The black triangles in Fig. 1 are site locations, and each site has three sectors. The red hexagon is called sector 1, to which the UE is connected. Green hexagons are active sectors which cause interference to the UE, while white hexagons are switched-off sectors.

The patterns are assumed to be periodic, i.e., expand to infinite. However we limited the plot on the figures keeping in mind that there should be enough interferers for sector 1 to model the real interference situation. In some patterns, there might be two or three configuration for the same number of active BSs. This is referred to as a pattern rotation and identified by the subscript letter X in the pattern symbol: $\mathsf{P}_\mathrm{X}(n/m)$; those patterns are enclosed in a rectangle. Those patterns represent either the same patterns or different sectors in the same pattern.

C. Sector-Level CSO Patterns

This level focuses on the number of active sectors at each BS site; these patterns are denoted as $\mathsf{P}(1, k/3)$, where k is the number of active sectors per site. The proportion of active sectors is $\rho = \frac{k}{3}$. There are three different patterns at this level: all sectors are active: $\mathsf{P}(1)$; two sectors are active: $\mathsf{P}(1, 2/3)$; and only one active sector: $\mathsf{P}(1, 1/3)$. No rotations are necessary at this level, as site-level patterns already contain all rotations. Fig. 2 illustrates the sector-level patterns that can be combined with each site-level pattern to form new patterns.

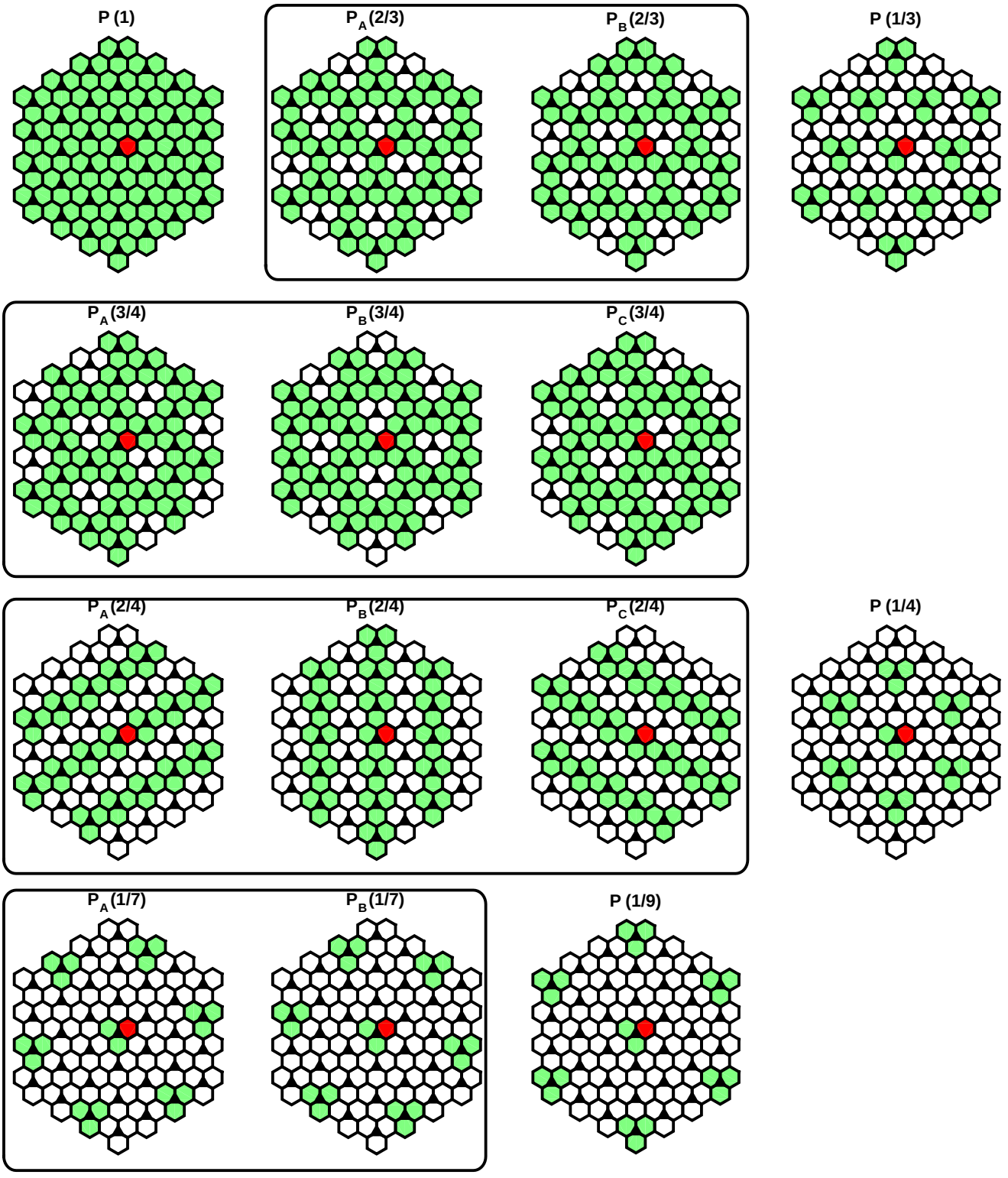

Figure 1. Site-level patterns. Black triangles are site locations, each site having three sectors. The red hexagon is sector 1 to which the UE is connected, green hexagons are active sectors which cause interference to the UE, while white hexagons are switched-off sectors. Patterns with the same number of active BSs but have different rotations are enclosed in a rectangle.

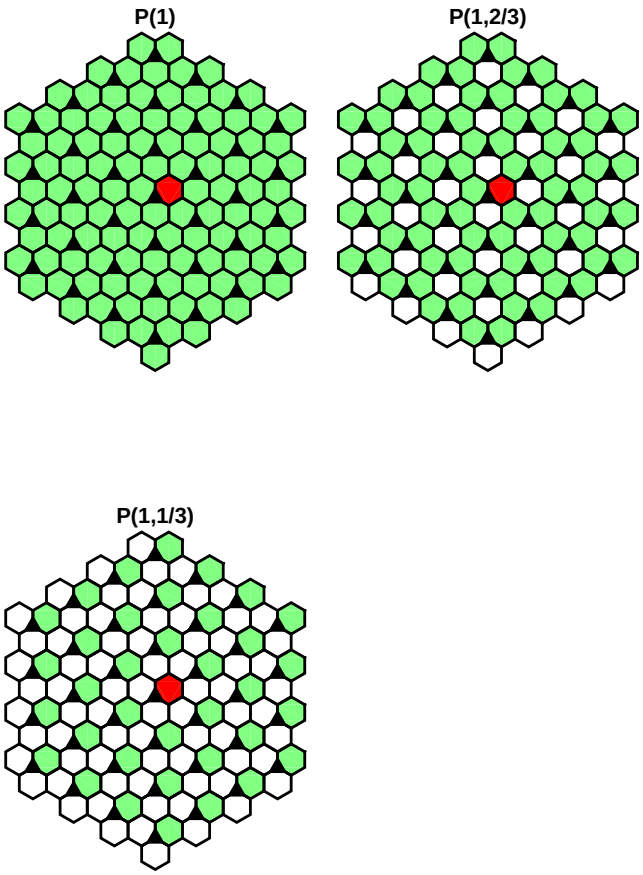

Figure 2. Sector-level patterns. All BSs are active and only the number of active sectors per BS is different.

D. Combining Sector-Level and Site-Level Patterns

Any site-level pattern can be combined with any sector-level pattern, in which case the active sectors are those resulting from the logical AND operation of the two patterns (there are 14×3 combinations). These patterns are denoted as $\mathsf{P}_{\mathrm{X}}(n/m, k/3)$, where the subscript X denotes the rotation of the pattern, the first term inside parenthesis is the site-level pattern, and the second term is the sector-level pattern. The proportion of active sectors is $\rho = |\mathsf{P}(n/m, k/3)| = \frac{nk}{3m} \in [0, 1]$.

In order to further illustrate this idea, we focus on two interesting examples. These examples introduce different patterns with the same proportion of active sectors.

1) One third of the sectors are active: In this example, we illustrate all the CSO patterns where one third of the sectors are active (i.e., $\rho = \frac{1}{3}$), namely: $\mathsf{P}(1, 1/3)$, $\mathsf{P}(1/3)$, $\mathsf{P}_{\mathrm{A}}(2/4, 2/3)$, $\mathsf{P}_{\mathrm{B}}(2/4, 2/3)$, and $\mathsf{P}_{\mathrm{C}}(2/4, 2/3)$. These patterns are illustrated in Fig. 3. It is worth mentioning that there are different rotations for the case of $\mathsf{P}(2/4, 2/3)$. Two of them, $\mathsf{P}_{\mathrm{A}}(2/4, 2/3)$ and $\mathsf{P}_{\mathrm{B}}(2/4, 2/3)$, represent a different sector in the same pattern, whereas $\mathsf{P}_{\mathrm{C}}(2/4, 2/3)$ is a different pattern.

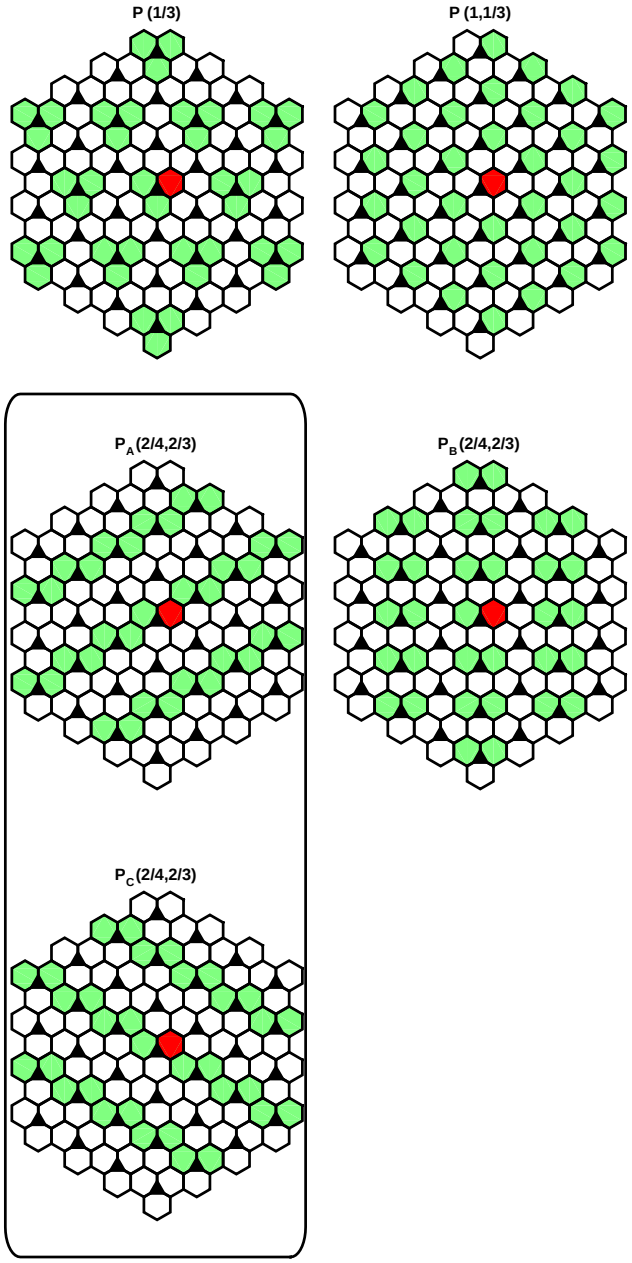

Figure 3. All patterns with $\rho = 1/3$. Patterns inside the rectangle represent different locations in the same pattern.

2) One sixth of the sectors are active: In this example, we illustrate all the CSO patterns where one sixth of the sectors are active (i.e., $\rho = \frac{1}{6}$), namely: $\mathsf{P}(1/4, 2/3)$, $\mathsf{P}_{\mathrm{A}}(2/4, 1/3)$, $\mathsf{P}_{\mathrm{B}}(2/4, 1/3)$ and $\mathsf{P}_{\mathrm{C}}(2/4, 1/3)$. These patterns are illustrated in Fig. 4. It is worth mentioning that there are different rotations for the case of $\mathsf{P}(2/4, 1/3)$. Two of them, $\mathsf{P}_{\mathrm{B}}(2/4, 1/3)$ and $\mathsf{P}_{\mathrm{C}}(2/4, 1/3)$, are the same patterns, whereas $\mathsf{P}_{\mathrm{A}}(2/4, 1/3)$, is a different pattern.

We will investigate the first example in detail in Section V.

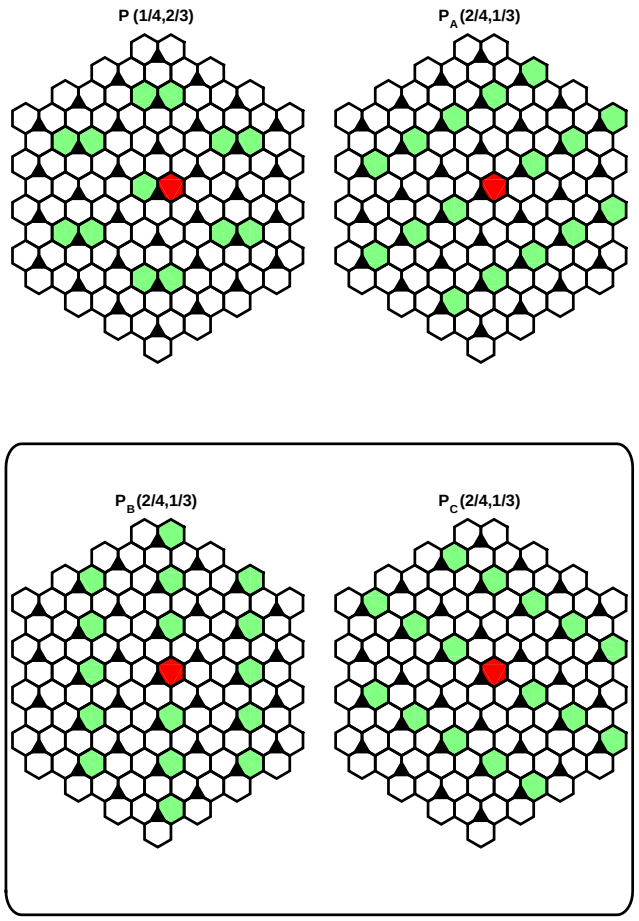

Figure 4. All patterns with $\rho = 1/6$. Patterns inside the rectangle are isomorphic.

E. Number of Users in the Network

The average number of UEs per system sector is

$$\mathbb{E}\{\rho\, N\} \cong \frac{W}{\mathbb{E}\{R\}}\eta_{eq}\,\rho. \tag{12}$$

In order to find the average number of UEs supported by the network, one simply multiplies (12) by the total number of sectors in the network. Thus, $\eta_{eq}\,\rho$ is proportional to the average number of UEs supported by the network.

F. Power Saving in Sector Switch-Off

In CSO literature, the amount of energy saving is assumed to be directly proportional to the number of switched-off sectors (or BSs). This is a valid assumption, especially as the power consumption of a BS is highly independent of its load [4], [5]. It is worth investigating the relationship between the site switch-off and sector switch-off. In a typical LTE network, each BS has three sectors; however, switching off one sector is not necessarily equivalent to one third of energy saving. This is because there is the common hardware that is shared among the three sectors at each site, such as cooling and baseband processing; as illustrated in Fig. 5.

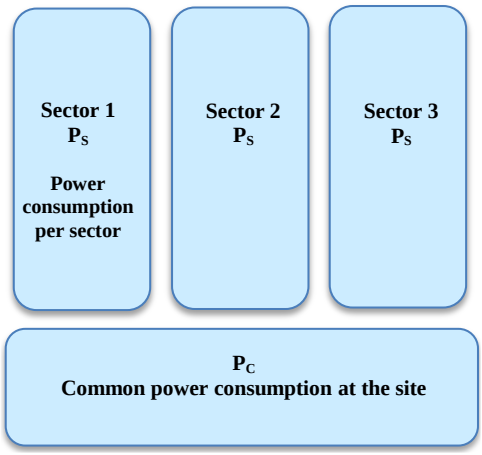

Figure 5. Power consumption at a site $(P_{site}) = P_C + 3P_S$, when all sectors are active.

In this section, we provide the equation to compare the power consumption of site-level CSO pattern $\mathsf{P}(n/3m)$ and of the the pattern $\mathsf{P}(n/m, 1/3)$ with $1/3$ active sectors per site. The average power consumption at each site of pattern $\mathsf{P}(n/m, k/3)$ is

$$P_{site} = \frac{n}{m}(P_C + kP_S). \tag{13}$$

This equation is useful to determine which one to choose between two patterns with the same ρ.

We compare two patterns with the same proportion of active sectors $\rho = \frac{n}{3m}$. Then for pattern $\mathsf{P}(n/m, 1/3)$, we have

$$P_{site,1} = \frac{n}{m}(P_C + 1P_S), \tag{14}$$

and for pattern $\mathsf{P}(n/3m)$, we have

$$P_{site,2} = \frac{n}{3m}(P_C + 3P_S). \tag{15}$$

We compare the consumed power per UE, and find the breakpoint:

$$\frac{P_{site,1}}{N_1} = \frac{P_{site,2}}{N_2}. \tag{16}$$

we substitute (5):

$$\frac{P_{site,1}}{\eta_{eq,1}W/\mathbb{E}\{R\}} = \frac{P_{site,2}}{\eta_{eq,2}W/\mathbb{E}\{R\}}. \tag{17}$$

$$\frac{P_{site,1}}{P_{site,2}} = \frac{\eta_{eq,1}}{\eta_{eq,2}}. \tag{18}$$

$$\frac{(1+\alpha)}{(\frac{1}{3}+\alpha)} = \frac{1}{\delta}. \tag{19}$$

where, $\delta = \eta_{eq,2}/\eta_{eq,1}$ and $\alpha = P_S/P_C$.

Then we can find the breakpoint

$$\alpha^* = \frac{\delta - \frac{1}{3}}{1-\delta}. \tag{20}$$

If $\alpha < \alpha^*$[1] then the site-level pattern $\mathsf{P}(n/3m)$ is more efficient; otherwise, the pattern $\mathsf{P}(n/m, 1/3)$ with $1/3$ active sectors is preferred.

[1]The value of α is known by the network operator.

Table III
Simulation Parameters for Urban Microcell (UMi) and Urban Macrocell (UMa) Scenarios

Parameter	Assumption	
ITU scenario	UMi	UMa
Cellular layout	Hexagonal	
Antenna pattern	120°-3 sectors	
Inter-site distance	200 m	500 m
BS antenna height	10 m	25 m
Cell transmitted power	41 dBm	46 dBm
Carrier frequency (f_c)	2.5 GHz	
UE distribution	random and uniform	
Probability of indoor UEs	0.5	0
UE noise figure	5 dB	
BS noise figure	7 dB	
Thermal noise	-174 dBm/Hz	
Shadowing spread (LOS)	3 dB	4 dB
Shadowing spread (NLOS)	4 dB	6 dB
SINR range	[-7, 18] dB	
Traffic type	full queue	

Similar calculations can be done for the case of 2/3 active sectors; however, we will find in the next section that those patterns are not favourable in terms of energy efficiency.

IV. Simulation

In this paper, we consider the downlink for a cellular network with hexagonal layout. We simulate two ITU scenarios, the Urban Micro-cell (UMi) and the Urban Macro-cell (UMa), according to the evaluation guidelines of [26]. The simulation parameters are listed in Table III.

Sector 1 (the red hexagon) is chosen as a typical sector, and we consider all UEs that get the best downlink SINR when connected to sector 1. Other active sectors (green hexagons) will cause interference to those UEs. All UEs are uniformly and independently distributed over the entire network area.

The patterns are assumed to be periodic, i.e., expand to infinite. However we limited the number of BSs in the network keeping in mind that there should be enough interferers for sector 1 to model the real interference situation For each CSO pattern, we simulate a large number of UEs to estimate the ESE according to (6), as well as P_o and $\mathbb{C}\mathrm{oV}\{1/\eta\}$. Results are summarized in Table IV for both the UMi and the UMa scenarios.

Fig. 6 compares the performance of different CSO patterns. The x-axis is proportional to the average number of UEs that can be supported by the network, as given by (12). The y-axis is the proportion of active sector which is proportional to the total energy saving. Different markers indicate the number of active sectors per BS site. The reference line gives locations where the performance of the network is scaled proportionally with respect to the fully active network $\mathsf{P}(1)$. The trend is that patterns with all sector active are fall close to the reference line, while patterns with two active sectors per BS fall to the left of the reference line (perform worse). Interestingly, patterns with one active sector per BS fall to the right of the line (perform better). For example, consider the case of $\rho = 0.33$: the number of active sectors is reduced to one third; however, the average number of UEs that can be supported by pattern $\mathsf{P}(1, 1/3)$ is only reduced to 48.5%, almost half of full capacity. The yellow staircase curve shows the operational region based on the best performing pattern for any given ρ. This curve can be used by operators to select the best pattern to follow to support a given user density demand.

In order to make the study complete, we compare the performance of regular CSO patterns with irregular static (offline) CSO [15] and also with dynamic (online) CSO [11]. Note that the values for irregular static CSO are obtained according to the simulation parameters indicated in [15], but with a uniform UE distribution. As we can conclude from the figure, regular CSO patterns perform very comparably, and even better at some points, to the irregular static CSO. For the case of dynamic CSO, the values in the curve are obtained according to the simulation parameters indicated in [11], but with a uniform UE distribution. It is worth mentioning that the simulation parameters used in [11] are not entirely compliant with our simulation parameters. One fundamental difference is that in [11] UEs are served in a way that maximizes the aggregate network capacity, i.e., UEs with high spectral efficiency are provided with large bandwidth, while UEs with low Spectral efficiency might be ignored. In our simulation, UEs are served in a first-come first-served basis. Thus [11] can be considered as an upper bound for both CSO and admission control design.

V. Case Study

In this section, we further investigate all the patterns with $\rho = 1/3$, shown in Fig. 3 (the first example from Section III-D). All the figures in this section are for the UMi scenario; however, we find that the UMa scenario shows a similar trend.

A. SINR Distribution

Each CSO pattern results in a different spatial distribution of the SINR of a typical UE connected to sector 1, as seen in Fig. 7.

Fig. 8 shows the effect of the chosen patterns on the resulting cumulative distribution function (CDF) of the SINR for UEs connected to sector 1. To validate our simulation platform, we also included the average CDF results obtained from the WINNER+ project using multiple simulation tools [24]. As shown in the figure, the SINRs obtained from the pattern $\mathsf{P}(1)$ produces a CDF that closely matches the WINNER+ results. Note that pattern $\mathsf{P}(1)$ is the case where all cells are active, i.e., without CSO.

It is worth mentioning that there is a high improvement in the SINR in pattern $\mathsf{P}(1, 1/3)$, where only one sector is active per site. This improvement is due to the significant reduction in the number of nearby interferers. However, the values of SINR are truncated at 18 dB [25]; these higher SINR values might be of interest in future systems that allow for higher constellations.

Table IV
Equivalent Spectral Efficiency.

	UMi				UMa			
Pattern	η_{eq}	$\eta_{eq}\cdot\rho$	P_o	$\mathbb{C}\text{oV}\left\{\frac{1}{\eta}\right\}$	η_{eq}	$\eta_{eq}\cdot\rho$	P_o	$\mathbb{C}\text{oV}\left\{\frac{1}{\eta}\right\}$
$\mathsf{P}(1)$	1.53	1.53	0.00	0.75	1.37	1.37	0.00	0.63
$\mathsf{P}(1,2/3)$	1.36	0.91	0.10	0.75	1.36	0.91	0.00	0.66
$\mathsf{P}(1,1/3)$	2.22	0.74	0.00	0.82	2.06	0.69	0.08	0.86
$\mathsf{P}_{\mathrm{A}}(2/3)$	1.57	1.04	0.00	0.71	1.42	0.95	0.08	0.70
$\mathsf{P}_{\mathrm{A}}(2/3,2/3)$	1.37	0.61	0.07	0.74	1.30	0.58	0.14	0.76
$\mathsf{P}_{\mathrm{A}}(2/3,1/3)$	2.03	0.45	0.02	0.94	1.65	0.37	0.70	0.97
$\mathsf{P}_{\mathrm{B}}(2/3)$	1.48	0.99	0.00	0.78	1.21	0.81	0.02	0.70
$\mathsf{P}_{\mathrm{B}}(2/3,2/3)$	1.35	0.60	0.03	0.72	1.32	0.59	0.00	0.70
$\mathsf{P}_{\mathrm{B}}(2/3,1/3)$	2.13	0.47	0.00	0.93	1.79	0.40	0.63	0.93
$\mathsf{P}(1/3)$	1.44	0.48	0.76	0.84	1.36	0.45	0.82	0.83
$\mathsf{P}(1/3,2/3)$	1.28	0.29	0.15	0.78	1.17	0.26	1.35	0.80
$\mathsf{P}(1/3,1/3)$	1.92	0.21	0.14	0.95	1.48	0.16	3.41	0.97
$\mathsf{P}_{\mathrm{A}}(3/4)$	1.57	1.18	0.00	0.72	1.45	1.09	0.06	0.64
$\mathsf{P}_{\mathrm{A}}(3/4,2/3)$	1.36	0.68	0.09	0.74	1.33	0.66	0.18	0.75
$\mathsf{P}_{\mathrm{A}}(3/4,1/3)$	2.18	0.54	0.00	0.91	1.91	0.48	0.21	0.94
$\mathsf{P}_{\mathrm{B}}(3/4)$	1.58	1.18	0.00	0.71	1.35	1.01	0.09	0.70
$\mathsf{P}_{\mathrm{B}}(3/4,2/3)$	1.39	0.69	0.00	0.71	1.32	0.66	0.06	0.71
$\mathsf{P}_{\mathrm{B}}(3/4,1/3)$	2.23	0.56	0.02	0.88	1.73	0.43	0.30	0.94
$\mathsf{P}_{\mathrm{C}}(3/4)$	1.46	1.10	0.03	0.80	1.19	0.90	0.07	0.72
$\mathsf{P}_{\mathrm{C}}(3/4,2/3)$	1.33	0.67	0.07	0.76	1.29	0.65	0.02	0.70
$\mathsf{P}_{\mathrm{C}}(3/4,1/3)$	1.93	0.48	0.02	0.94	1.69	0.42	0.88	0.97
$\mathsf{P}_{\mathrm{A}}(2/4)$	1.66	0.83	0.02	0.71	1.43	0.71	0.10	0.71
$\mathsf{P}_{\mathrm{A}}(2/4,2/3)$	1.35	0.45	0.04	0.73	1.17	0.39	0.75	0.78
$\mathsf{P}_{\mathrm{A}}(2/4,1/3)$	1.75	0.29	0.30	1.03	1.36	0.23	2.64	0.97
$\mathsf{P}_{\mathrm{B}}(2/4)$	1.45	0.73	0.02	0.77	1.27	0.63	0.13	0.75
$\mathsf{P}_{\mathrm{B}}(2/4,2/3)$	1.41	0.47	0.01	0.73	1.42	0.47	0.09	0.75
$\mathsf{P}_{\mathrm{B}}(2/4,1/3)$	2.00	0.33	0.01	0.90	1.67	0.28	1.41	0.97
$\mathsf{P}_{\mathrm{C}}(2/4)$	1.43	0.72	0.00	0.77	1.34	0.67	0.00	0.68
$\mathsf{P}_{\mathrm{C}}(2/4,2/3)$	1.25	0.42	0.11	0.74	1.19	0.40	0.75	0.74
$\mathsf{P}_{\mathrm{C}}(2/4,1/3)$	2.04	0.34	0.01	0.90	1.58	0.26	1.16	0.94
$\mathsf{P}(1/4)$	1.55	0.39	0.00	0.69	1.45	0.36	0.39	0.75
$\mathsf{P}(1/4,2/3)$	1.26	0.21	0.35	0.76	1.14	0.19	2.80	0.83
$\mathsf{P}(1/4,1/3)$	1.74	0.14	0.54	0.98	1.42	0.12	5.66	0.98
$\mathsf{P}_{\mathrm{A}}(1/7)$	1.23	0.18	0.93	0.77	1.16	0.17	6.03	0.83
$\mathsf{P}_{\mathrm{A}}(1/7,2/3)$	1.07	0.10	2.55	0.78	1.02	0.10	10.11	0.81
$\mathsf{P}_{\mathrm{A}}(1/7,1/3)$	1.44	0.07	4.45	1.04	1.34	0.06	15.08	1.02
$\mathsf{P}_{\mathrm{B}}(1/7)$	1.24	0.18	0.75	0.77	1.13	0.16	5.61	0.81
$\mathsf{P}_{\mathrm{B}}(1/7,2/3)$	1.09	0.10	2.71	0.78	1.07	0.10	9.02	0.81
$\mathsf{P}_{\mathrm{B}}(1/7,1/3)$	1.48	0.07	4.87	1.05	1.39	0.07	13.81	1.04
$\mathsf{P}(1/9)$	1.20	0.13	1.21	0.78	1.16	0.13	8.53	0.84
$\mathsf{P}(1/9,2/3)$	1.08	0.08	4.65	0.79	1.04	0.08	13.26	0.82
$\mathsf{P}(1/9,1/3)$	1.41	0.05	8.46	1.06	1.32	0.05	18.68	1.01

B. Number of Users per Sector

We now compare the number of supported UEs per active sector for all patterns with $\rho = 1/3$. After calculating η_{eq} and $\mathbb{C}\text{oV}\{1/\eta\}$ for each pattern, we assume a constant rate demand of 500 kbps and a system bandwidth of 10 MHz, resulting in $W/\mathbb{E}\{R\} = 20$ and $\mathbb{C}\text{oV}\{R\} = 0$, and we find the number of UEs that a typical sector can support, see Fig. 9.

Results show that the $\mathsf{P}(1,1/3)$ pattern can support the most UEs (44.5 UEs) per sector on average (which is also the median (50%)), and about 33 UEs 97.5% of the time (according to (11)). The distribution of the number of UEs closely follows a Gaussian distribution as expected from the analysis in Section III-A3.

C. Energy Efficiency Aspects

Based on the calculations in Section III-F, we can find the breakpoint that indicates which pattern is better in terms of energy efficiency per UE. While the patterns with 2/3 active sectors are never advantageous, the pattern $\mathsf{P}(1,1/3)$ is advantageous with respect to pattern $\mathsf{P}(1/3)$ as long as $P_S/P_C > \alpha = 0.8922$, as found from (20).

VI. Conclusion

CSO is a promising approach for more energy-efficient cellular networks. In this paper, we classified the CSO approaches, investigated in detail 42 different regular CSO patterns, and presented them in a systematic way. Furthermore, this paper was the first to investigate sectorized regular CSO patterns. The performance of different CSO patterns was compared using only one parameter. The distribution of the number of users supported was found to be close to Gaussian with a variance estimated using one additional parameter. The maximum number of supported users was obtained from patterns where one sector out of three is active at a site. In many cases, the performance of regular CSO patterns is comparable to that of a benchmark irregular static CSO. Moreover, although a benchmark dynamic CSO outperforms the regular CSO patterns, it is still reasonable to employ the regular CSO patterns because of their simplicity and scalability.

Regular CSO patterns are conceptually simple; and can be characterized systematically both statistically and geometrically. Location regularity of CSO patterns provides the advantages of: 1- ensures that interferer cells are as far

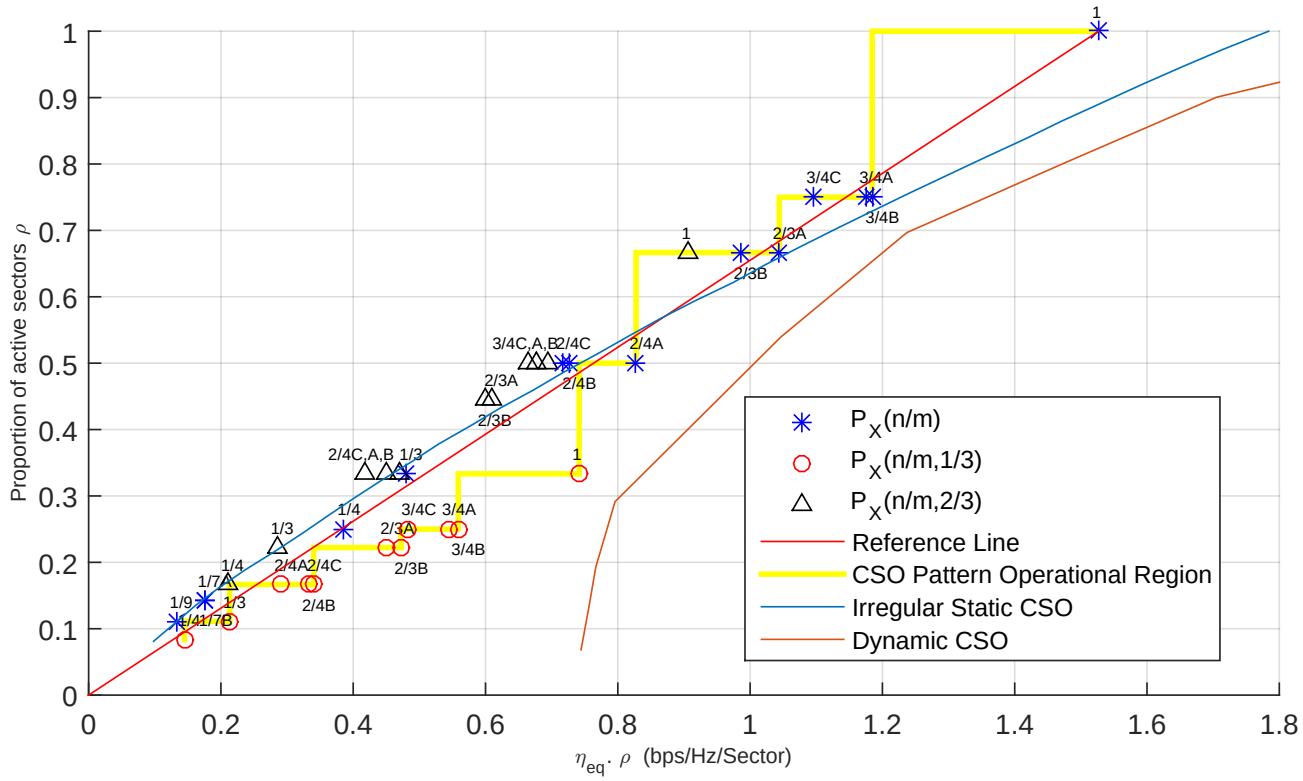

Figure 6. Comparison of the performance of different patterns and other CSO schemes for the UMi scenario. The x-axis is proportional to the average number of UEs supported by the network. The y-axis is proportional to the total energy saving. Different markers indicate the number of active sectors. The reference line gives locations where the performance of the network is scaled proportionally with respect to the fully active network $\mathsf{P}(1)$. The operational region curve follows the best performing pattern for any given ρ. The irregular static CSO is a benchmark from [15], while the dynamic CSO is a bench mark from [11]. Patterns with outage $P_o > 2\%$ are not included.

as possible, 2- allows for a realistic interference modeling, 3- minimizes the coverage holes, and 4- more energy-efficient for users in the uplink transmission as users do not transmit at full power, because there is always a nearby cell.

References

[1] J. G. Andrews, S. Buzzi, W. Choi, S. V. Hanly, A. Lozano, A. C. Soong, and J. C. Zhang, "What will 5G be?" *IEEE J. Sel. Areas Commun.*, vol. 32, no. 6, pp. 1065–1082, June 2014.

[2] Z. Hasan, H. Boostanimehr, and V. K. Bhargava, "Green cellular networks: A survey, some research issues and challenges," *IEEE Commun. Surveys Tuts.*, vol. 13, no. 4, pp. 524–540, 4th quarter 2011.

[3] I. Humar, X. Ge, L. Xiang, M. Jo, M. Chen, and J. Zhang, "Rethinking energy efficiency models of cellular networks with embodied energy," *IEEE Network*, vol. 25, no. 2, pp. 40–49, Mar. 2011.

[4] T. Beitelmal and H. Yanikomeroglu, "A set cover based algorithm for cell switch-off with different cell sorting criteria," in *Proc. IEEE International Conference on Communications Workshops (ICC)*, June 2014, pp. 641–646.

[5] D. González, H. Yanikomeroglu, M. Garcia-Lozano, and S. Ruiz Boque, "A novel multiobjective framework for cell switch-off in dense cellular networks," in *Proc. IEEE International Conference on Communications (ICC)*, June 2014, pp. 2641–2647.

[6] L. Budzisz, F. Ganji, G. Rizzo, M. Marsan, M. Meo, Y. Zhang, G. Koutitas, L. Tassiulas, S. Lambert, B. Lannoo, M. Pickavet, A. Conte, I. Haratcherev, and A. Wolisz, "Dynamic resource provisioning for energy efficiency in wireless access networks: A survey and an outlook," *IEEE Commun. Surveys Tuts.*, vol. 16, no. 4, pp. 2259–2285, 4th quarter 2014.

[7] K. C. Tun and K. Kunavut, "An overview of cell zooming algorithms and power saving capabilities in wireless networks," *KMUTNB: International Journal of Applied Science and Technology*, vol. 7, no. 3, pp. 1–13, July 2014.

[8] Z. Niu, Y. Wu, J. Gong, and Z. Yang, "Cell zooming for cost-efficient green cellular networks," *IEEE Commun. Mag.*, vol. 48, no. 11, pp. 74–79, Nov. 2010.

[9] F. Alaca, A. Bin Sediq, and H. Yanikomeroglu, "A genetic algorithm based cell switch-off scheme for energy saving in dense cell deployments," in *Proc. IEEE Global Communications Conference Workshops (GLOBECOM)*, Dec. 2012, pp. 63–68.

[10] A. Guo and M. Haenggi, "Spatial stochastic models and metrics for the structure of base stations in cellular networks," *IEEE Trans. Wireless Commun.*, vol. 12, no. 11, pp. 5800–5812, Nov. 2013.

[11] A. Alam, L. Dooley, and A. Poulton, "Traffic-and-interference aware base station switching for green cellular networks," in *Proc. IEEE International Workshop on Computer Aided Modeling and Design of Communication Links and Networks (CAMAD)*, Sept. 2013, pp. 63–67.

[12] M. Marsan, L. Chiaraviglio, D. Ciullo, and M. Meo, "Switch-off transients in cellular access networks with sleep modes," in *Proc. IEEE International Conference on Communications Workshops (ICC)*, June 2011, pp. 1–6.

[13] S. Kokkinogenis and G. Koutitas, "Dynamic and static base station management schemes for cellular networks," in *Proc. IEEE Global Communications Conference (GLOBECOM)*, Dec. 2012, pp. 1–6.

[14] F. Han, Z. Safar, W. Lin, Y. Chen, and K. Liu, "Energy-efficient cellular network operation via base station cooperation," in *Proc. IEEE International Conference on Communications (ICC)*, June 2012, pp. 4374–4378.

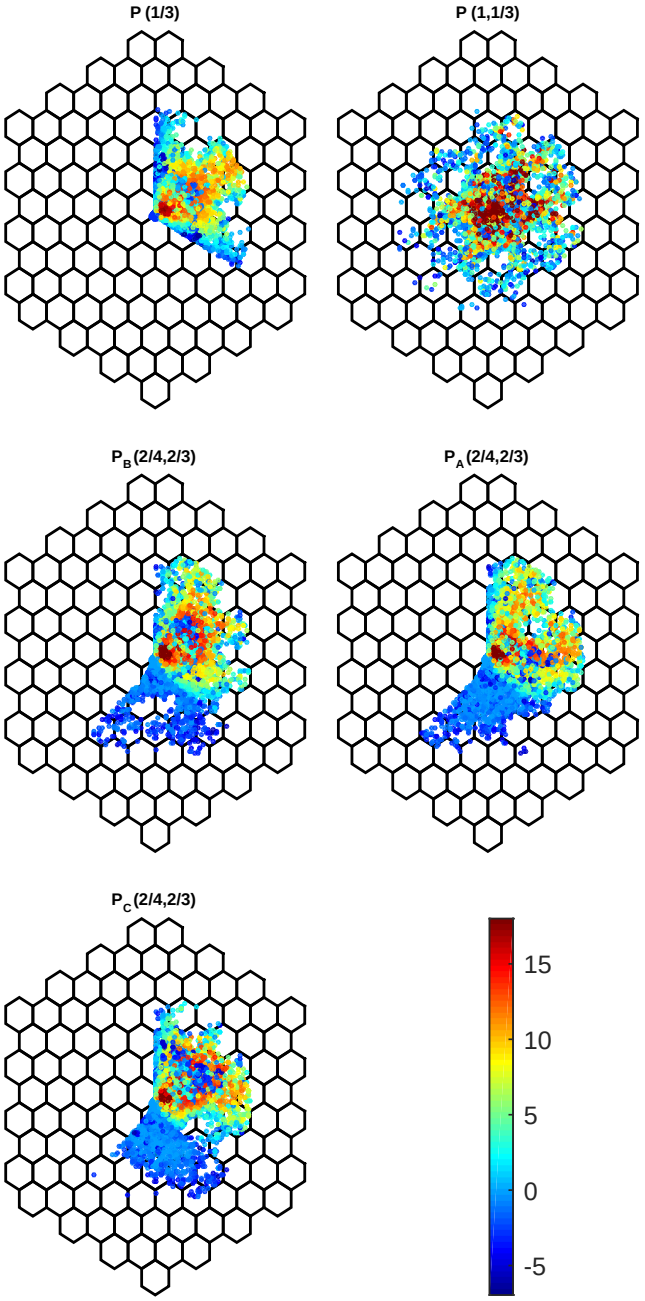

Figure 7. Spatial distribution of the SINR of a typical UE connected to sector 1, for patterns in Fig. 3, for the UMi scenario (the UMa scenario shows a similar trend). The UE is connected to the sector that results in the highest downlink SINR.

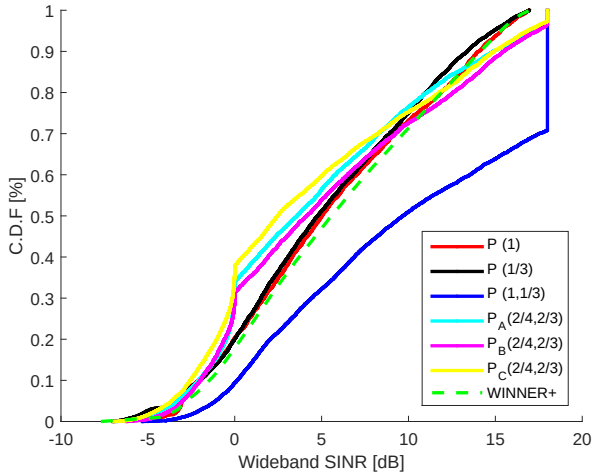

Figure 8. CDFs of SINR for patterns in Fig. 3 for the UMi scenario, with WINNER+ calibration for the fully active network (pattern P(1)).

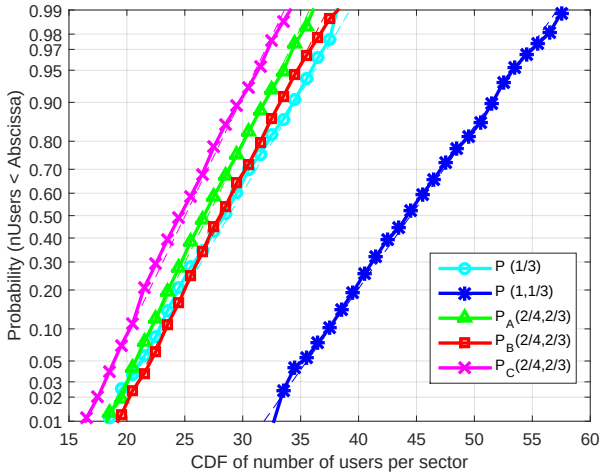

Figure 9. CDFs of the number of UEs supported for patterns in Fig. 3, when R is fixed and $W/R = 20$, for the UMi scenario. The y-axis is transformed so that the Gaussian distribution appears as a straight line.

[15] D. González, J. Hämäläinen, H. Yanikomeroglu, M. García-Lozano, and G. Senarath, "A novel multiobjective cell switch-off method with low complexity for realistic cellular deployments," *arXiv preprint arXiv:1506.05595v1*, 2015.

[16] L. Suárez, L. Nuaymi, and J.-M. Bonnin, "Energy-efficient BS switching-off and cell topology management for macro/femto environments," *Computer Networks*, vol. 78, pp. 182–201, Nov. 2014.

[17] L. Chiaraviglio, D. Ciullo, M. Meo, and M. A. Marsan, "Energy-efficient management of UMTS access networks," in *Proc. IEEE International Teletraffic Congress (ITC)*, Sept. 2009, pp. 1–8.

[18] X. Weng, D. Cao, and Z. Niu, "Energy-efficient cellular network planning under insufficient cell zooming," in *Proc. IEEE Vehicular Technology Conference (VTC Spring)*, May 2011, pp. 1–5.

[19] A. Kumar and C. Rosenberg, "Energy and throughput trade-offs in cellular networks using base station switching," *IEEE Trans. Mobile Comput.*, vol. 15, no. 2, pp. 364–376, Feb. 2016.

[20] L. B. Le, "QoS-aware BS switching and cell zooming design for OFDMA green cellular networks," in *Proc. IEEE Global Communications Conference (GLOBECOM)*, Dec. 2012, pp. 1544–1549.

[21] M. Marsan, L. Chiaraviglio, D. Ciullo, and M. Meo, "Optimal energy savings in cellular access networks," in *Proc. EEE International Conference on Communications Workshops (ICC)*, June 2009, pp. 1–5.

[22] "Telecommunication management; study on energy savings management (ESM)," 3rd Generation Partnership Project (3GPP), TR 32.826, Apr. 2010.

[23] S. M. Ross, *Introduction to Probability Models*, Burlington, MA, USA, 2007.

[24] "Calibration for IMT-Advanced Evaluations," CELTIC/CP5-026 Project WINNER+, Munich, Germany, Tech. Rep., May 2010.

[25] D. Bultmann, T. Andre, and R. Schoenen, "Analysis of 3GPP

LTE-Advanced cell spectral efficiency," in *Proc. IEEE International Symposium on Personal Indoor and Mobile Radio Communications (PIMRC)*, Sept. 2010, pp. 1876–1881.

[26] ITU-R, "Report ITU-R M.2135-1; guidelines for evaluation of radio interface technologies for IMT-Advanced," 2009.